

Hydraulic Permeabilities of PET and Nylon 6 Electrospun Fiber Webs

Kyung Hwa Hong, Tae Jin Kang

School of Materials Science & Engineering, Seoul National University, Seoul 151-742, South Korea

Received 17 December 2004; accepted 7 April 2005

DOI 10.1002/app.22651

Published online in Wiley InterScience (www.interscience.wiley.com).

ABSTRACT: The morphological and hydraulic properties of electrospun fiber webs were investigated and compared with those of spunbond nonwoven fabrics. In this study, poly(ethylene terephthalate) (PET), hydrophobic polymer, and nylon 6, with some hydrophilic groups (amide groups), were used as the polymer materials to prepare spunbonds and electrospun fiber webs. The water permeabilities of PET and nylon 6 spunbonds followed the Darcy's law, but those of PET and nylon 6 electrospun fiber webs showed properties that deviated from the Darcy's law. On the other hand, the wicking phenomenon was observed in both nylon 6

spunbond and electrospun fiber webs, but no such phenomenon was observed in PET spunbond and electrospun fiber webs. The water vapor transport rates of PET and nylon 6 electrospun fiber webs were higher than those of PET and nylon 6 spunbonds. © 2006 Wiley Periodicals, Inc. *J Appl Polym Sci* 100: 167–177, 2006

Key words: electrospinning; nanofiber web; nylon 6; PET; hydraulic permeability; wicking; vapor transport rate; Darcy's law; Washburn's equation

INTRODUCTION

Unlike the conventional fiber-spinning techniques, such as wet spinning, dry spinning, melt spinning, and gel spinning, which are capable of producing polymer fibers with diameters down to the micrometer range, electrostatic spinning or "electrospinning" is a process capable of producing polymer fibers in the nanometer diameter range. In the electrospinning process, a polymer solution or melt is placed into a syringe with a millimeter-sized nozzle and is subjected to electric fields of several kilovolts. Under the applied electrostatic force, the polymer is ejected from the nozzle, whose diameter is reduced significantly as it is transported to and deposited on a collector, which also serves as the ground for the electrical charges. Depending on the specific polymer being used and the processing conditions of electrospinning, a range of fabric properties, such as strength, weight, and porosity, can be achieved.

And also, much smaller fiber diameters and increased surface areas are accessible through the electrospinning technique, as compared with currently available textile fibers.¹ Therefore, current emphasis of researches is to exploit such mechanical properties of the electrospun nanofibers and focus on determining appropriate conditions for electrospinning various

polymers and copolymers for eventual applications, including multifunctional membranes, biomedical structural elements, protective shields in special fabrics, filter media for submicron particles in separation industry, composite reinforcement, and structures for nanoelectronic machines among others.²

Berkland et al.³ reported that woven mats of submicron electrospun poly(D,L-lactide-co-glycolide) (PLG) fibers used as vascular grafts offer improved permeability and flexibility when compared with conventional PLG films, and thus by controlling fiber diameter and density (threads per area), the performance of the graft can be further improved. Norris et al.⁴ have stated in their article that considering the well-known fact that the rate of electrochemical reactions is proportional to the surface area of the electrode, they were interested in exploiting the high surface-to-volume ratio of electrospun fibers to develop porous polyaniline electrodes. Also, Gibson et al.¹ reported that electrospun fiber webs would provide good resistance to the penetration of the chemical and biological warfare agents in aerosol form, while still allowing significant water vapor transport to promote evaporative cooling of the body in a protective clothing.

Therefore, if the fluid permeability and the wicking property as well as the vapor and gas transport properties of the electrospun fiber web were thoroughly characterized, it would be useful in applying the electrospun fiber web to specific industrial items, such as filtering materials, electrodes, biomedical membranes, and others. Thus, we prepared nylon 6 as well as poly(ethylene terephthalate) (PET) nanofiber webs

Correspondence to: K. H. Hong (hkh713@snu.ac.kr).

Contract grant sponsor: Ministry of science and technology.

TABLE I
Characteristics of PET and Nylon 6 Chips

PET chip	
Intrinsic viscosity	0.652 ± 0.007
D-EG (wt %)	0.9 ± 0.2
COOH (eq/TON)	40 ± 10
Color	Semi dull
Nylon 6 chip	
Relative viscosity (η_{rel})	2.73
Molecular weight (M_w)	22,910
Moisture regain (ppm)	500
Color	Semi dull

through electrospinning process, and then investigated the morphological and hydraulic properties, such as water permeability, wicking, and moisture transport property of the electrospun fiber webs. Also the experimental as well as analytical results of the electrospun fiber webs were compared with those of the conventional spunbond nonwoven fabrics.

EXPERIMENTAL

Materials and chemicals

PET chips and nylon 6 chips for preparing nanofiber webs were obtained from Toray Sehan Co., Korea, and Hyosung Co., Korea, respectively. PET spunbond and nylon 6 spunbond also were obtained from Toray Sehan Co., Korea and Ahahi Kasei Fiber Co., Japan,

respectively. The characteristics of the PET and nylon 6 chips are shown in Table I. The chemicals such as formic acid [HCOOH], trichloroacetic acid [CCl₃COOH], and dichloromethane [CH₂Cl₂] used as solvents for dissolving the nylon 6 and PET polymer are all of reagent grade and were obtained from Ducksan Pure Chemical Co., Korea.

Preparation of PET and nylon 6 nanofiber webs

PET polymer solution of 16 wt % was prepared by the dissolution of PET chips in trichloroacetic acid (50 wt %) and dichloromethane (50 wt %) solvent mixture. Nylon 6 polymer solution was prepared by dissolving nylon 6 chips in formic acid. The electrospinning apparatus used in this study is shown in Figure 1. The hypodermic syringe used in this experiment had a capillary tip diameter of 19 gauge. A positive potential was applied to the PET and nylon 6 polymer solution by connecting a copper wire to the metal capillary tip, and the potential differences between the tip and the counter electrode (collector) used to electrospin the polymer solution were 14 kV (PET) and 25 kV (nylon 6), respectively. A rotating drum covered with aluminum foil, placed 10 cm below the capillary tip, was used to collect the electrospun fiber material.

Evaluation

The porosities of electrospun fiber webs and spunbonds were measured by the helium porosimeter

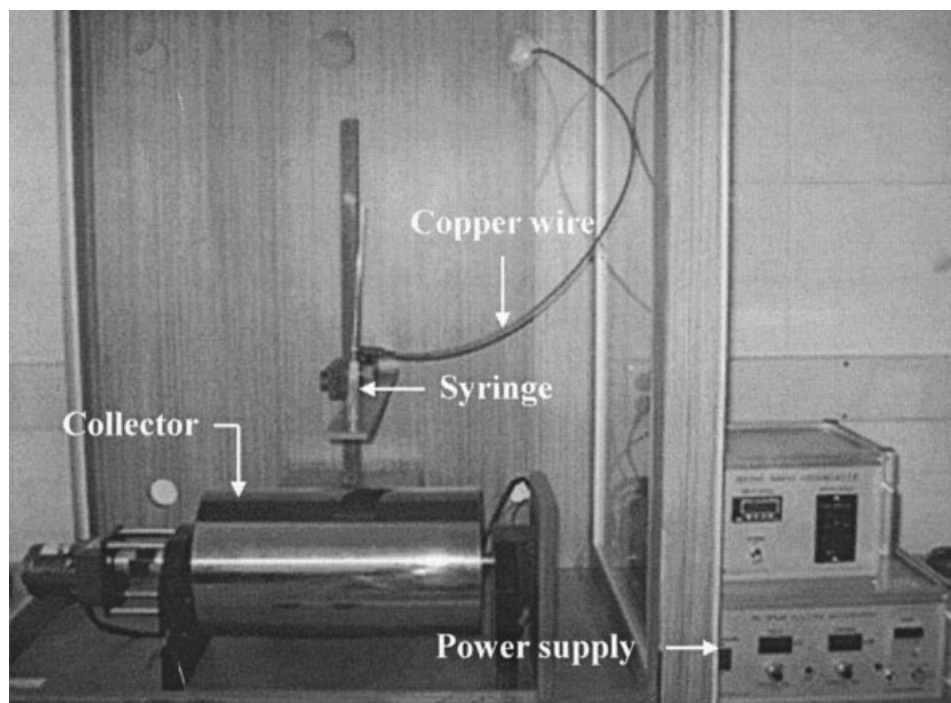


Figure 1 System setup for electrospinning process.

(Harbert Engineering, Tulsa, OK). The instrument operates on the principle of Boyle's law, which states that for an ideal gas in a closed system the product of pressure and volume remains constant at constant temperature. Porosity values were determined as follows:

$$\text{Porosity, } \phi = \frac{(V_b - V_f)}{V_b} = 1 - \frac{V_f}{V_b} \quad (1)$$

where, V_b is the bulk volume of the nonwoven fabrics and V_f is the fiber volume of the nonwoven fabrics.

The liquid extrusion method was developed to evaluate the pore size/pore size distribution of nonwoven matrix, following an established method. Before the measurements, fabric samples were presaturated with deionized water and were placed on the porous plate in the chamber, which was pressured stepwise by controlling the compressed air input. The liquid inside the samples was extruded under the specified pressure differences, which were recorded and converted into effective radius (r) by the following Young-Laplace equation [eq. (2)].⁵

$$r = \frac{2\gamma \cos\theta}{\Delta P} \quad (2)$$

where, ΔP is the differential pressure, γ is the surface tension of the liquid, and θ is the contact angle of the liquid.

The in-plane permeability was measured according to the ASTM F316 test method by using the liquid permeability tester (CFP-1200-AEL, Porous Materials Inc.). The flow of liquid through a sample is measured by the distance a column of liquid drops in relation to time and pressure. This method gives reproducible results, even for hydrophobic materials, as pressure can be applied up to 200 psi to the liquid column to force the liquid through the sample.

The liquid wicking rate was measured according to the ISO 9073-6 standard test method. The capillary method measures the rate of vertical capillary rise in a specimen strip suspended with the lower end dipped in a thin layer of diluted water. The height of capillary rise of the liquid after 10, 30, 60, and 300 s was recorded, and if the capillary rise was not a uniform straight line, the highest point was recorded.

The moisture vapor permeability was measured based on the KS K0574 standard test method. The material to be tested was sealed into the mouth of an impermeable cup containing a vapor pressure regulator, dessicant (CaCl_2). The cup was then placed in an environmental chamber, whose temperature was $(40 \pm 2)^\circ\text{C}$ and relative humidity was $(90 \pm 5)\%$, and a constant vapor pressure difference was maintained across the sample. Once equilibrium was attained (af-

TABLE II
Characteristics of PET Spunbond and Electrospun Fiber Webs, and Nylon Spunbond and Electrospun Fiber Webs

	Fiber mean diameter (nm)	Web density (g/m^2)	Thickness (mm)
PET electrospun	842	40.8	0.2426
Nylon electrospun	967	37	0.1594
PET spunbond	16,53	79.6	0.2904
Nylon spunbond	14,66	50	0.3268

ter 12 h), the vapor flow was determined from the steady change in cup weight with time. The moisture permeability, P ($\text{g m}^{-2}/12 \text{ h}$) for the experiment was then calculated from eq. (3).

$$P = \frac{10(a_2 - a_1)}{S} \quad (3)$$

where, $a_2 - a_1$ is the weight difference (mg) of the sample material after 12 h, and S is the moisture transport area (cm^2).

RESULTS AND DISCUSSION

Morphologies

Porous materials are important in many scientific and engineering applications, such as catalysis, hydrology, tissue engineering, membrane separation processes, wetting and drying processes, powder technology, contaminant transport in soil and aquifers, and enhanced oil recovery.⁶ The prediction of the effective or macroscopic transport properties in the porous materials is a long-standing problem of great fundamental and practical significance.⁷ Therefore, we investigated the morphological and moisture-transport properties of the electrospun fiber web, one of the most porous materials, in an attempt to probe some of its possible applications.

In this study, the PET and nylon 6 spunbonds, and the PET and nylon 6 electrospun fiber webs were prepared in such a way that they had similar morphologies. We investigated the hydraulic properties of electrospun fiber webs and also compared the properties with those of spunbonds as a function of polymer material properties. Therefore, PET, hydrophobic polymer, and nylon 6, with some hydrophilic groups of amide groups in their polymer backbone, were used as the polymer materials to prepare the spunbonds as well as electrospun fiber webs. More specifications of the spunbonds and electrospun fiber webs are depicted in Table II.

Figures 2 and 3 show the morphologies of PET spunbond and PET electrospun fiber web, and nylon 6 spunbond and nylon 6 electrospun fiber webs, respec-

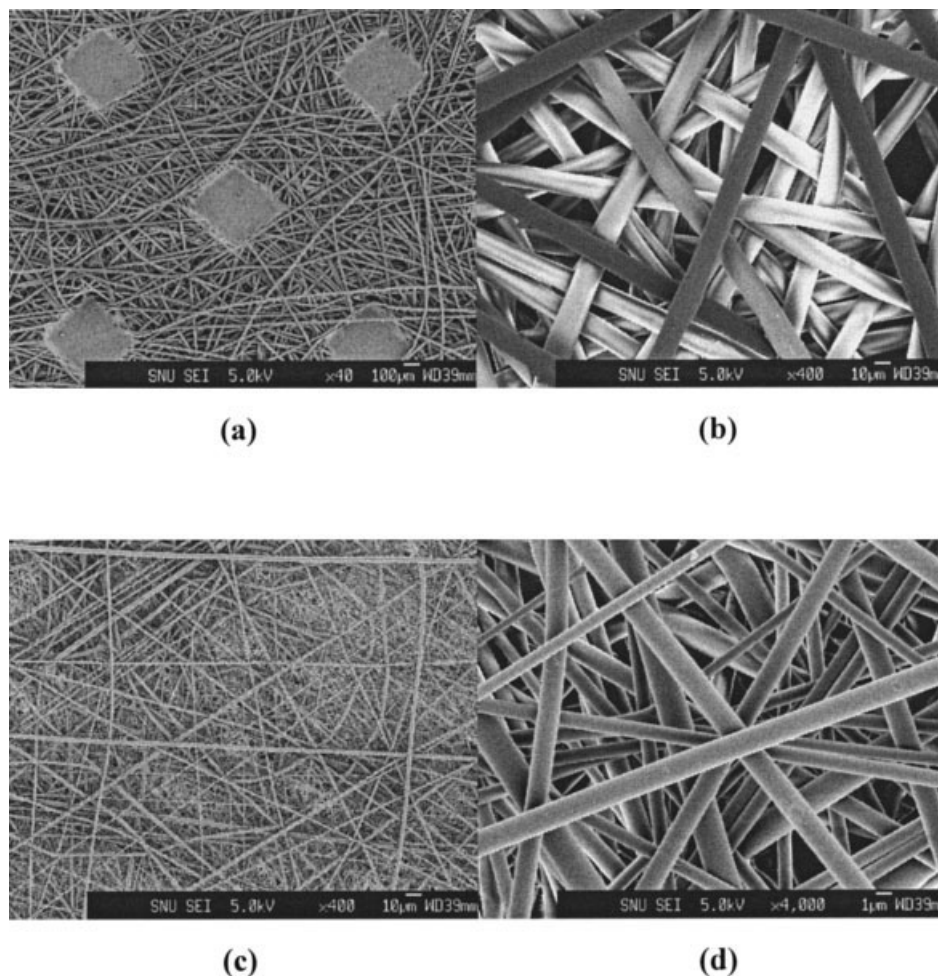


Figure 2 SEM photographs of PET spunbond ((a): $\times 40$; (b): $\times 400$) and PET electrospun fiber web ((c): $\times 400$; (d): $\times 4000$).

tively. The average diameters of PET and nylon 6 electrospun fibers are respectively ~ 842 nm and ~ 967 nm, and these scales are almost 1/17 times as large as those of PET and nylon 6 spunbonds (PET spunbond fibers, $16.53 \mu\text{m}$; nylon 6 spunbond fibers, $14.66 \mu\text{m}$). Also, it was observed that the distribution of fiber diameters in the PET and nylon 6 electrospun fiber webs were wider than in the PET and nylon 6 spunbonds. It was thought that during the electrospinning process, the whipping motion of the ejected polymer solution or fiber caused by electric force is very chaotic and unstable. On the other hand, both the spunbond fibers and electrospun fibers are randomly distributed to form a nonwoven mat with good integrity. However, although the spunbonds had some heat-adhered parts as shown in Figures 2(a) and 3(a), we did not consider their effects in this study.

Pore size characteristics of nonwovens

The theoretical prediction of macroscopic transport properties of porous media is made difficult by its

complex dependence on composition and structure of pore space. An idealized but extremely popular scheme to present the complex geometry of a porous medium is to map it onto a collection of interconnected pore bodies and throats. In this scheme, proposed first by Fatt,⁸ the narrow throats offer most of the resistance to flow whereas the wider pore bodies contribute the most to overall porosity of the pore space. Therefore, we characterized the pore sizes and porosities of PET spunbond and electrospun fiber webs, and nylon 6 spunbond and electrospun fiber webs.

Figure 4 exhibits the average pore size of the PET spunbond and electrospun fiber webs as well as nylon 6 spunbond and electrospun fiber webs. It was observed that the differences between the average pore sizes of spunbonds and electrospun fiber webs were smaller than the differences between their average fiber diameters. It was thought that the spunbond webs were additively compressed by the posttreatment, which imposed the heat-adhered parts in the spunbond webs. However, the electrospun fibers were

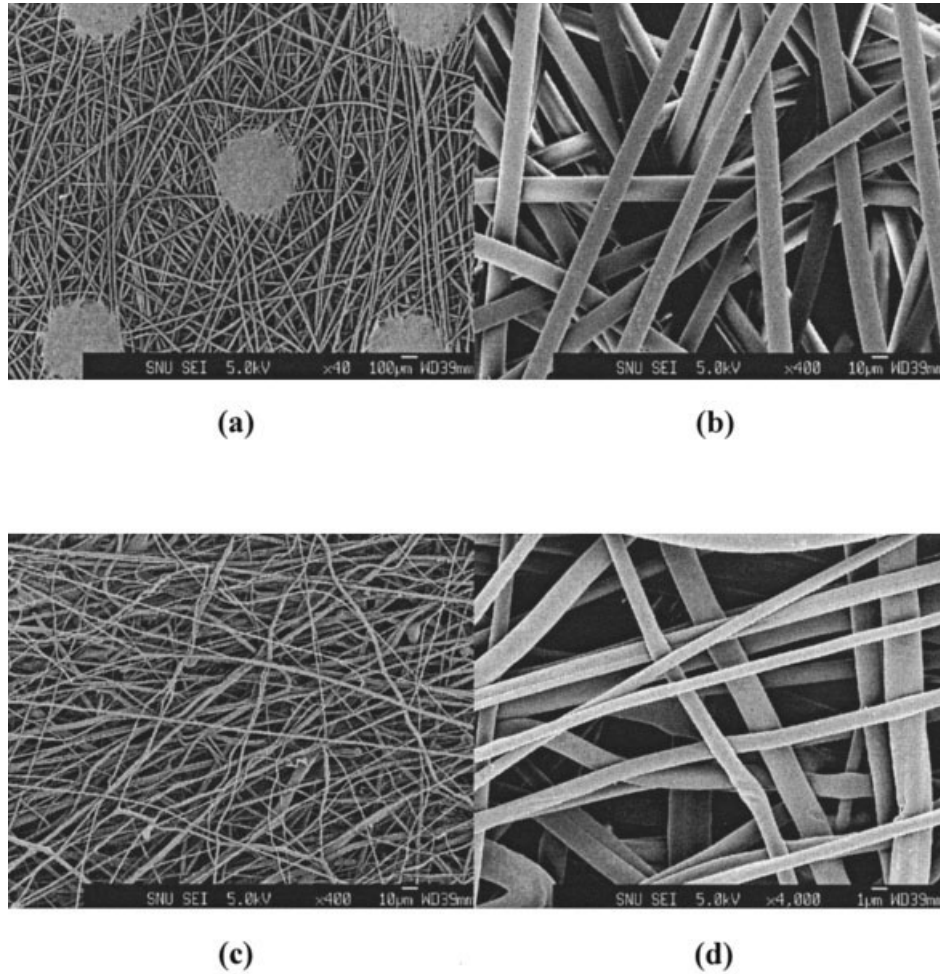


Figure 3 SEM photographs of nylon 6 spunbond ((a): $\times 40$; (b): $\times 400$) and nylon 6 electrospun fiber web ((c): $\times 400$; (d): $\times 4000$).

only entangled by the simple force of fiber deposition, and the slightly adhered parts were caused when the fibers had met each other before sufficient solidification. Figure 5 displays that all the nonwovens have similar porosities. It was assumed that the pore sizes of the spunbonds were larger than those of the electrospun fiber webs; however, the spunbonds had fewer number of pores than the electrospun fiber web had. Even though the porosities of spunbond and electrospun fiber web remain unchanged, the pore sizes of electrospun fiber webs are much smaller than those of spunbonded fiber webs, and this has a profound effect on the water vapor transport phenomenon.

Hydraulic permeabilities

Many engineering applications use materials normally referred to as porous media because a porous medium is any material permeable to liquid and gaseous flows. The nanofiber web prepared by an

electrospinning process is one of the prospective porous materials, and it has a distinct, very fine pore-body structure. Thus, it was expected that the fluid transport properties of the electrospun fiber webs were different from those of the conventional nonwoven fabrics, and we investigated the moisture transport properties of electrospun fiber webs and compared the results with those of spunbond nonwoven fabrics.

The liquid permeability is a material property related to flow resistance through the material as described by Darcy's law (eq. (4)), which depends on the properties of both the porous medium itself as well as the fluids percolating through it. Darcy's law shows that the volumetric flow rate is a function of the flow area, elevation, fluid pressure, and proportionality constant.

$$V = -\frac{K}{\mu} \cdot \frac{dP}{dh} \quad (4)$$

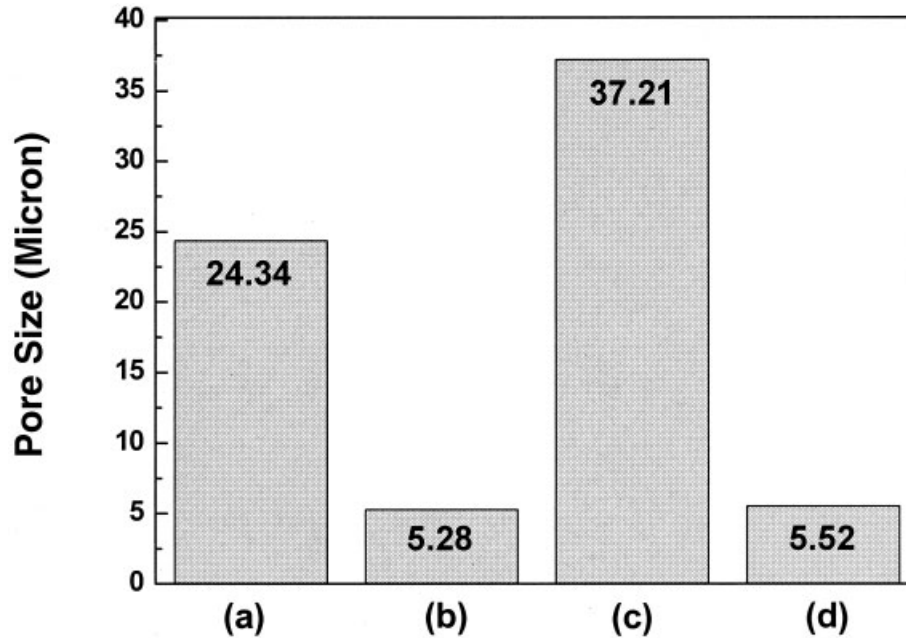


Figure 4 Average pore sizes of (a) PET spunbond, (b) PET electrospun fiber web, (c) nylon 6 spunbond, and (d) nylon 6 electrospun fiber web.

where, V is the fluid velocity, μ is the viscosity of the fluid, K is the permeability of the medium, P is the fluid pressure, and h is the coordinate axis along the suction direction.

It may be stated in several different forms depending on the flow conditions. Since its discovery, it has been found valid for any Newtonian fluid. Likewise, although it was established under saturated flow con-

ditions, it may be adjusted to account for unsaturated and multiphase flow.^{9,10} In the flow range, the pressure drop per unit length is found to be linear with respect to mass flow rate. The plots of the measured flow rate versus applied pressure gradient of PET spunbond and electrospun fiber webs, and nylon 6 spunbond and electrospun fiber webs are given in Figures 6 and 7. Both plots of PET spunbond [Fig. 6(a)]

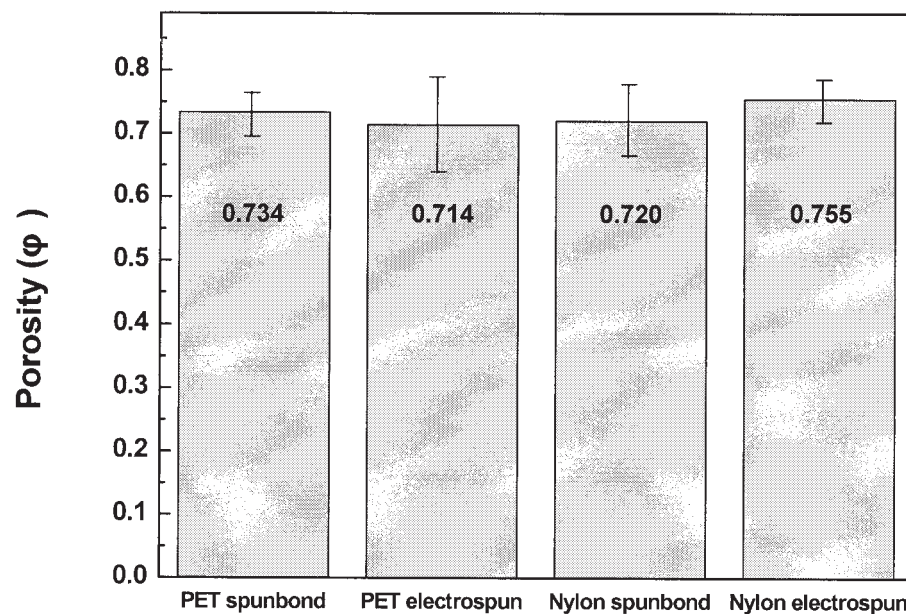


Figure 5 Porosity of (a) PET spunbond, (b) PET electrospun fiber web, (c) nylon 6 spunbond, and (d) nylon 6 electrospun fiber web.

and nylon 6 spunbond [Fig. 7(a)] are linear, showing that the water flows in PET and nylon 6 spunbonds were indeed in the range of validity of Darcy’s law. The permeability, K , value of nylon 6 spunbond (~0.323) is larger than that of PET spunbond (~0.220). This is because the average pore size of nylon 6 spunbond is larger than that of PET spunbond, as shown in Figure 4. Greene et al.¹¹ reported that migration rates within porous material was thought to be intimately connected to pore size.

However, the plots of PET electrospun fiber web [Fig. 6(b)] and nylon 6 electrospun fiber web [Fig. 7(b)] showed properties that deviated from the Darcy’s law. It was presumably thought that the PET and nylon 6 electrospun fiber webs were not permeable up to some specific hydraulic pressure points because of their extremely fine pore-body structures; however, they withstood till the points when the structures were ruptured (PET electrospun fiber web, >146.59 psi/mm; nylon 6 electrospun fiber web, >131.68 to 145.19 psi/mm).

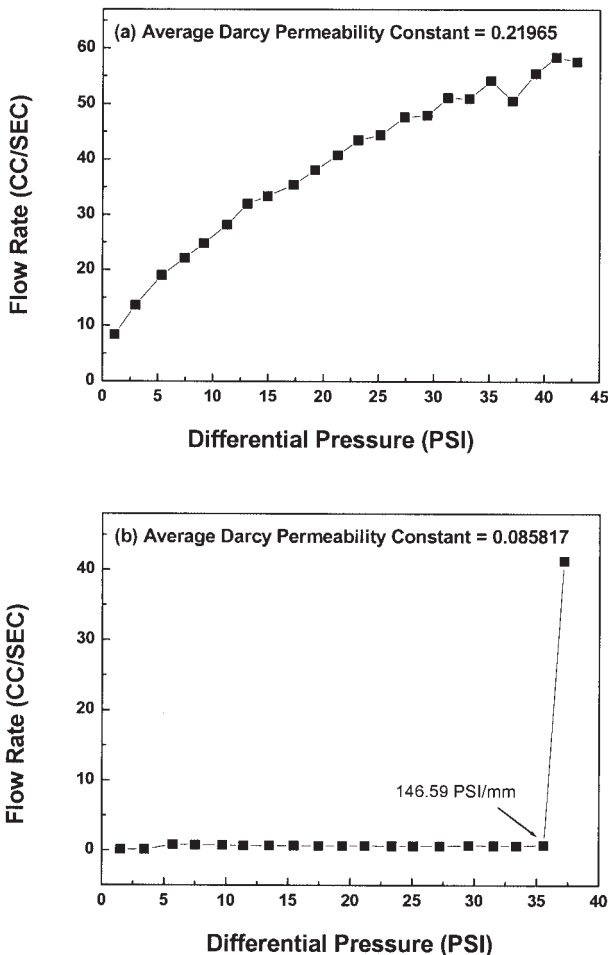


Figure 6 Water flow rate with differential pressures and average Darcy’s permeability constants of (a) PET spunbond and (b) PET electrospun fiber web.

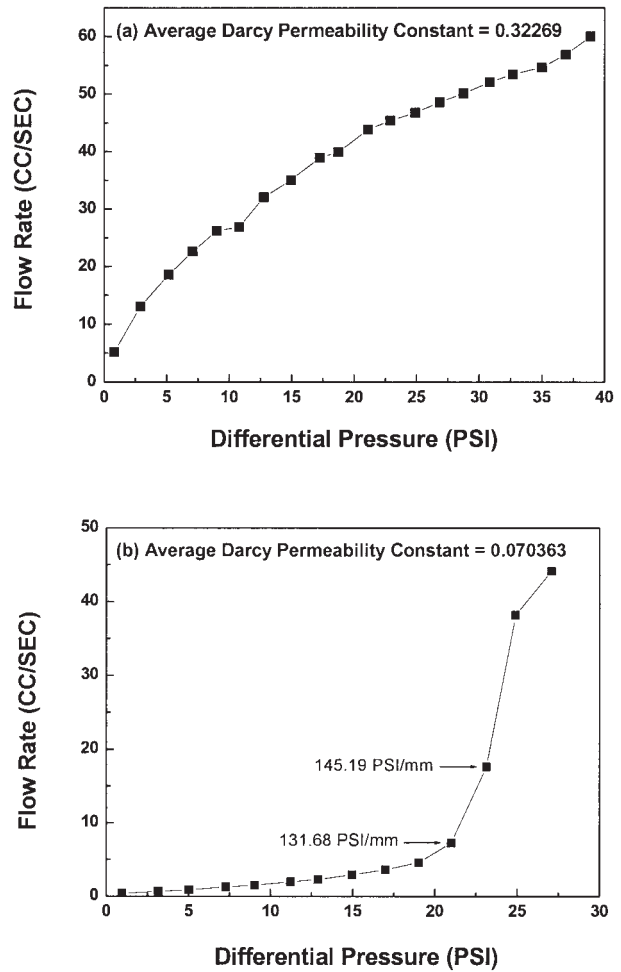


Figure 7 Water flow rate with differential pressures and average Darcy’s permeability constants of (a) nylon 6 spunbond and (b) nylon 6 electrospun fiber web.

On the other hand, nylon 6 electrospun fiber web is a little permeable below its specific pressure point causing the rupture of the structure, compared to PET electrospun fiber web. It was assumed that nylon 6 polymer has some hydrophilic groups (amide groups) in its polymer backbone and so the pore walls of the nylon 6 electrospun fibers are familiar with water. Because the linear Darcy’s law is known to break down if the flow becomes too slow, the interactions between the fluid and the pore walls become important. Examples occur during the slow movement of polar liquids or electrolytes in finely porous materials with high specific internal surface.¹²

Wetting and wicking properties of nonwovens

Wetting is the displacement of a fiber–air interface with a fiber–liquid interface. Wicking is the spontaneous flow of a liquid in a porous substrate, driven by capillary forces.¹³ Capillarity can be defined as the macroscopic motion of a fluid system under the influ-

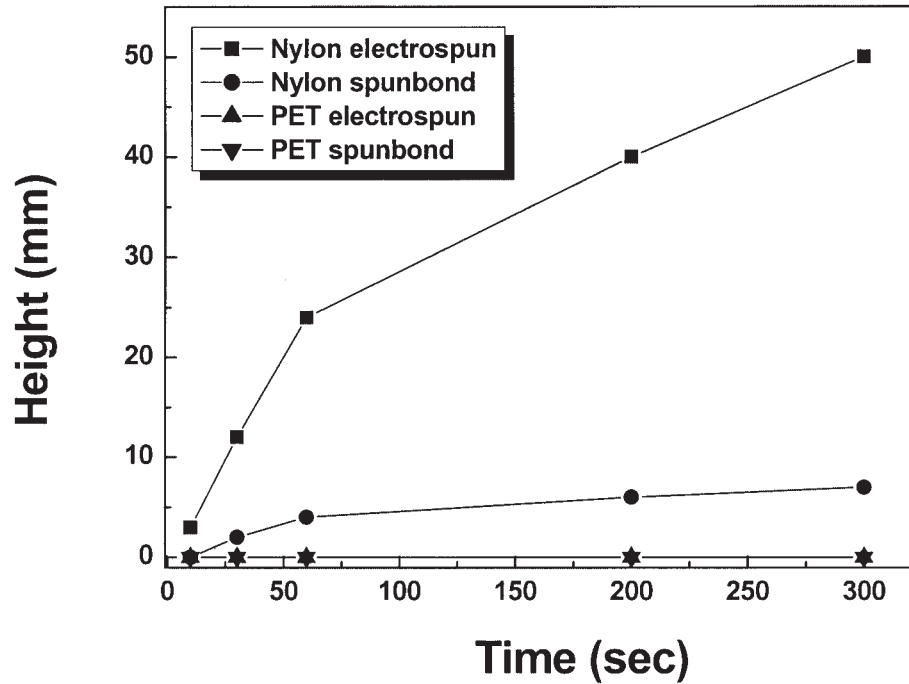


Figure 8 Liquid wicking rates of (■) nylon 6 electrospun fiber web, (●) nylon 6 spunbond, (▲) PET electrospun fiber web, and (▼) PET spunbond as a function of touching times with water.

ence of its own surface and interfacial forces. The capillary phenomena arise as a result of differences in pressure across a curved liquid–solid interface. The most important mechanisms causing flow in permeable media are viscous force, gravity force, capillarity force, and dispersion (diffusion).¹⁴ Several techniques can be used to measure the wicking and wetting in textile and paper applications. The first technique consists of weight variation measurements with a Wilhelmy balance during capillary wicking.¹⁵ A second alternative is the setting of liquid-sensitive sensor regularly along the porous medium.¹⁶ The third technique consists of observing and measuring the capillary flow of a colored liquid either when the sample is placed perpendicularly to a liquid bath or when a droplet of liquid spreads on a sample surface.¹⁷

In this study we characterized the wicking properties of PET spunbond and electrospun fiber web, and nylon 6 spunbond and electrospun fiber webs using the third technique mentioned earlier, as shown in Figure 8. The wicking phenomenon was observed in nylon 6 spunbond and nylon 6 electrospun fiber web, but no such phenomenon was observed in PET spunbond and PET electrospun fiber web. This could be explained as follows. It is well known that the speed, V , is the water adsorption height (h) divided by time (t), and the h is proportioned to differential pressure (ΔP) according to the Darcy's law [eq. (4)]. On the other hand, in case of hydrophobic porous substrate (PET nonwovens) the surface tension (γ) between the pore wall and water is too small and so the ΔP is also

very small according to the Young–Laplace equation [eq. (2)]. Therefore, although the time, t , is extended in case of PET nonwovens, the height reached by the liquid at the time hardly increases.

On the other hand, the rise of liquid with time in nylon 6 spunbond and nylon 6 electrospun fiber webs is given by the relation observed by Washburn's equation [eq. (5)]:

$$h^2 = \frac{r\gamma \cos\theta}{2\eta} \cdot t \quad (5)$$

where, h is the height reached by the liquid at time t , η is the viscosity of the liquid, and γ is the surface tension of the liquid, and $r = R_D^2/R_S$; this term in fiber networks means an equivalent radius of the capillary porous structure (R_D ; the mean hydrodynamic radius of pores, R_S ; the mean static radius of pores).¹⁸ Hence, h^2 -values must vary linearly with time, t .

$$h^2 = D \cdot t \quad (6)$$

where, the slope D is a capillary diffusion coefficient related to the size of the capillaries, r , and to the physicochemical characteristics of the liquid.¹⁹ Therefore, the D -value of nylon 6 electrospun fiber web is larger than that of nylon 6 spunbond, as shown in Figures 9 and 10. It was presumed that the average pore size (r) of electrospun fiber web is smaller than that of spunbond, and so ΔP and h of nylon 6 electro-

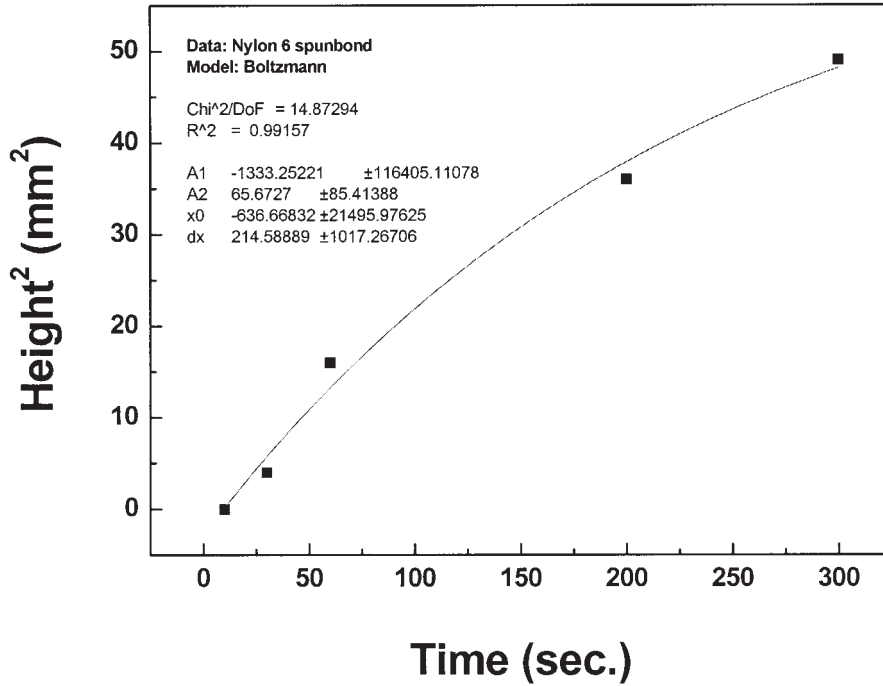


Figure 9 The squares of water absorption heights of nylon 6 spunbond as a function of time, *t*.

spun fiber web become larger than those of nylon 6 spunbond.

Moisture vapor transport properties

The process of moisture transport through porous substrate is an extremely complex phenomenon with

parallel/series moisture flow taking place in both the vapor and liquid phases.²⁰ In most hygroscopic building materials, capillary condensation will be initiated at a relative humidity of about 60%. At such levels of relative humidity some pores will be completely liquid-filled, while others will be partially filled, with condensation/reevaporation continuously occurring

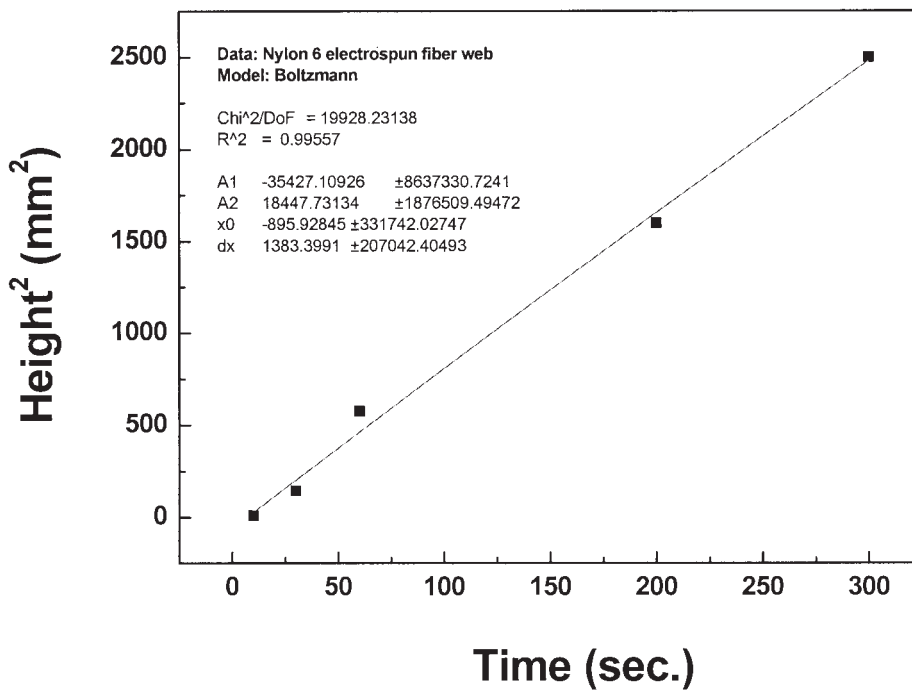


Figure 10 The squares of water absorption heights of nylon 6 electrospun fiber web as a function of time, *t*.

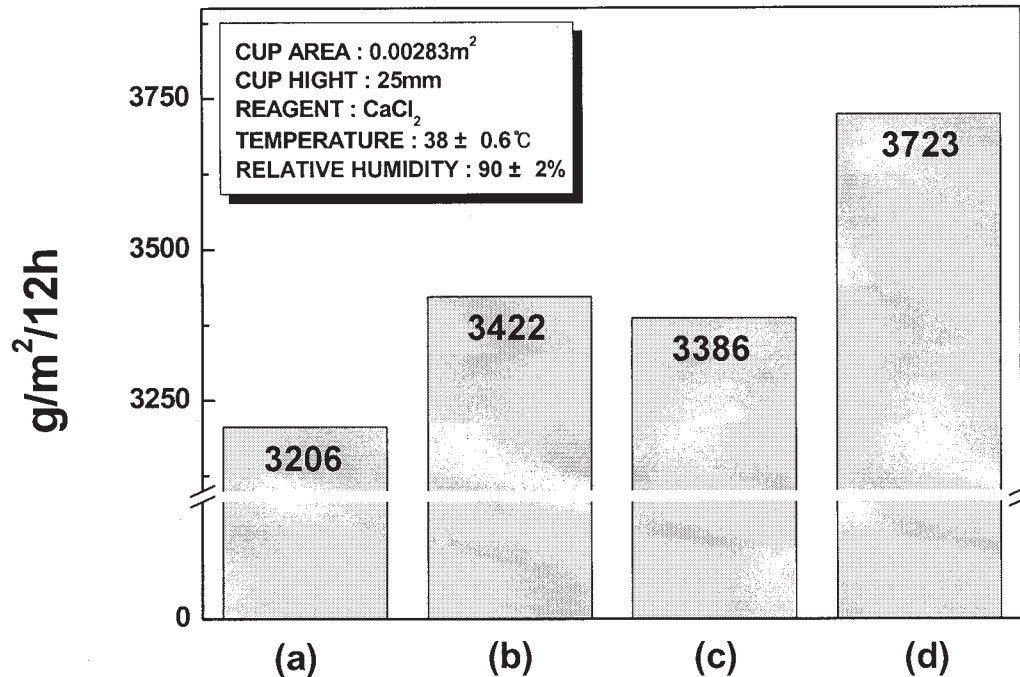


Figure 11 Moisture vapor permeability of (a) PET spunbond, (b) PET electrospun fiber web, (c) nylon 6 spunbond, and (d) nylon 6 electrospun fiber web measured by the inverted water method (ASTM E96–2000).

within the material voids. Therefore, the measurement carried out in this study, in fact, involves the determination of the total moisture flux through a sample under isothermal conditions. The total flux will include moisture transport both in the liquid and in the vapor state.²¹

On the other hand, the permeability of a gas, vapor, or liquid through a dense polymeric membrane can be described by the solution-diffusion model,²² equating the permeability, P , to the product of the diffusivity and solubility:

$$P = D \cdot S \quad (7)$$

where, D is the diffusion coefficient and S is the solubility coefficient. The magnitude of the permeability is determined by the diffusion rate (D), which is a kinetic parameter, and the solubility, a thermodynamic parameter accounting for the amount absorbed by the membrane. The combination of a high mobility for water (diffusivity) and a high solubility causes a high permeability for water compared with other penetrants.²³

Figure 11 shows the moisture vapor permeabilities of PET spunbond and electrospun fiber web, and nylon 6 spunbond and electrospun fiber web. It was observed that the vapor permeabilities of electrospun fiber webs are superior to those of the spunbonds. Gibson et al.¹ reported that electrospinning results in submicrometer-sized fibers laid down in a layer that has high porosity but very small pore size, and so the

nanofibers assemble into a membranelike structure that exhibits excellent moisture vapor transport, extremely low air permeability, and good aerosol particle protection. In particular, the vapor permeability of the nylon 6 electrospun fiber web was much increased than that of nylon 6 spunbond. It was thought that under the (90 ± 2)% of relative humidity (the experimental condition), moisture capillary condensation could have occurred in all the nonwoven fabrics, and so in case of nylon 6 electrospun fiber web, the effect of wicking would further increase the moisture vapor permeability.

Therefore, if the filaments composing the electrospun fiber web could have strong coherent forces among them by means of thermal or chemical treatment, it would be possible to obtain a new membrane with unique nature, which will thoroughly keep out water (liquid) but allow the transport of water vapor.

CONCLUSIONS

The morphological and hydraulic properties of electrospun fiber web were investigated and compared with those of spunbond nonwoven fabrics. PET, hydrophobic polymer, and nylon 6, with some hydrophilic groups (amide groups), were used as the polymer materials to prepare spunbonds and electrospun fiber webs. The hydraulic permeabilities of PET and nylon 6 spunbond followed the Darcy's law, but those of PET and nylon 6 electrospun fiber webs showed

properties that deviated from the Darcy's law. It was assumed that electrospun fiber webs were not permeable because of the fine pore sizes up to some specific hydraulic pressures (PET electrospun fiber web, about 146.59 psi/mm; nylon 6 electrospun fiber web, about 131.68–145.19 psi/mm); however, after those points, the structures ruptured. On the other hand, the wicking phenomenon was observed both in nylon 6 spunbond and in nylon 6 electrospun fiber web, but no such wicking phenomenon was observed in PET spunbond and PET electrospun fiber webs. It was thought that the pore walls of nylon 6 nonwovens were familiar to water because of the hydrophilic nature of amide bonds. In particular, the rise of liquid with time in nylon 6 spunbond and nylon 6 electrospun fiber webs are given by the relation observed by Washburn's equation; that is to say h^2 -values (the squares of water absorption heights of nonwoven substrates) varied linearly with time, t . The water vapor transport rate of PET and nylon 6 electrospun fiber webs were higher than those of PET and nylon 6 spunbonds. This is because the electrospun fiber web has smaller pore size distribution when compared with the conventional spunbonded fiber web even though both webs have the same level of porosity. Therefore, if the filaments composing the electrospun fiber web could have strong coherent forces among them by means of thermal or chemical treatment, it would be possible to obtain a new membrane with unique nature, which will thoroughly keep out water (liquid) but allow the transport of water vapor well.

This study was supported by the Ministry of Science and Technology through the National Research Laboratory at Seoul National University. The authors are grateful for this support.

References

1. Gibson, P.; Schreuder-Gibson, H.; Rivin, D. *Colloid Surf A: Physicochem Eng Aspect* 2001, 187/188, 469.
2. Frenot, A.; Chronakis, I. S. *Curr Opin Colloid Interface Sci* 2003, 8, 64.
3. Berkland, C.; Pack, D. W.; Kim, K. K. *Biomaterials* 2004, 25, 5649.
4. Norris, I. D.; Shakar, M. M.; Ko, F. K.; MacDiarmid, A. G. *Synth Met* 2000, 114, 109.
5. Bok, J. S. Masters' Thesis, Chungnam National University, 2001.
6. Singh, M.; Mohanty, K. K. *Chem Eng Sci* 2003, 58, 1.
7. Sahimi, M. *Rev Mod Phys* 1993, 65, 1393.
8. Fatt, I. *Trans AIME* 1956, 207, 160.
9. Friedrich, K.; Lutz, A.; Velten, K. *Compos Sci Technol* 1999, 59, 495.
10. William, R. R.; Harris, D. K. *Exp Therm Fluid Sci* 2003, 27, 227.
11. Greene, G.; Tannenbaum, R. *Appl Surf Sci* 2004, 233, 336.
12. <http://www.ica1.uni-stuttgart.de/local/WWW/papers/acp/node55.html>
13. Tavisto, M.; Kuisma, R.; Pasila, A.; Hautala, M. *Ind Crop Prod* 2003, 18, 25.
14. Chwastiak, S. J. *Colloid Interface Sci* 1973, 42, 298.
15. Heieh, Y. L.; Yu, B. *Text Res J* 1992, 62, 677.
16. Ito, H.; Muraoka, Y. *Text Res J* 1993, 63, 414.
17. Perwuelz, P.; Mondon, C.; Cazé, C. *Text Res J* 2000, 70, 333.
18. Perwuelz, A.; Casetta, M.; Caze, C. *Polym Test* 2001, 20, 553.
19. Ferrero, F. *Polym Test* 2003, 22, 571.
20. Rose, D. A. *Br J Appl Phys* 1963, 14, 491.
21. Mclean, R. C.; Galbraith, G. H.; Sanders, C. H. *Build Res Pract* 1990, 18, 82.
22. Baker, R. W.; Wijmans, J. G.; Athayde, A. L.; Daniels, R.; Ly, J. H.; Le, M. *J Membr Sci* 1999, 137, 159.
23. Metz, S. J. Ph.D. Thesis, Twente University, 2003.